



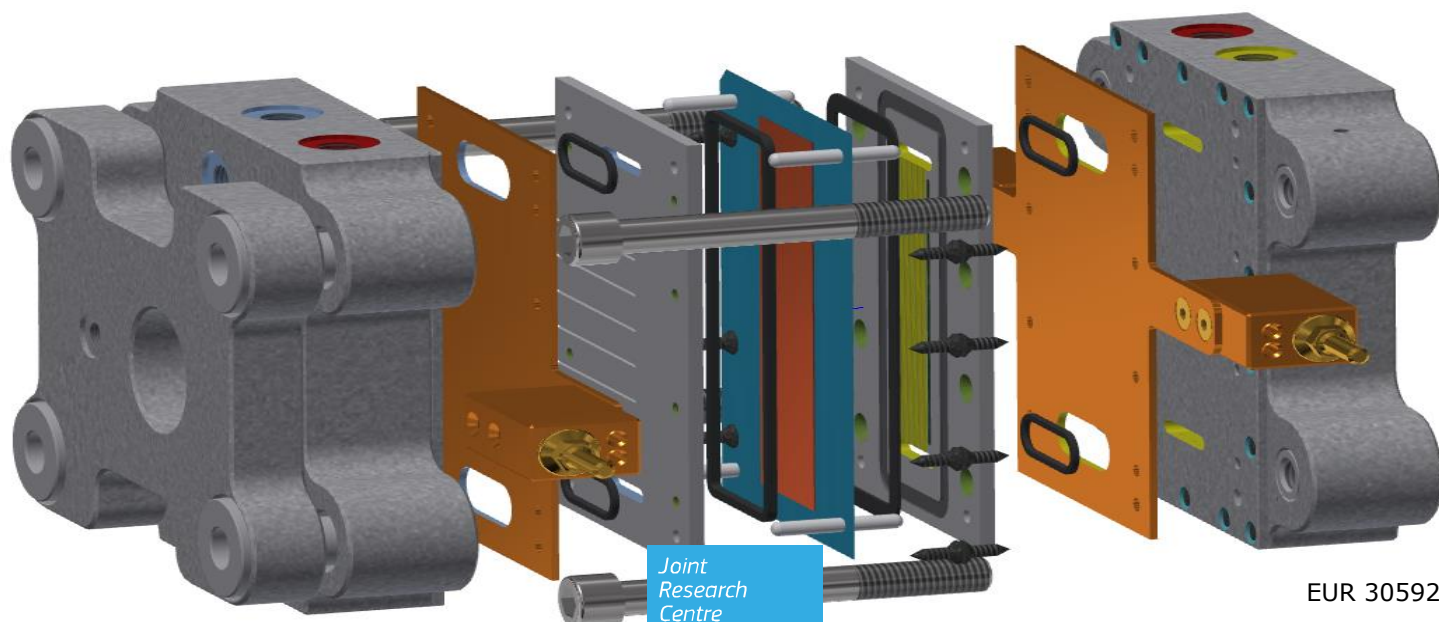
European
Commission

JRC TECHNICAL REPORT

Development of reference hardware for harmonised testing of PEM single cell fuel cells

Bednarek, T, Tsotridis, G

2021



EUR 30592 EN



This publication is a Technical report by the Joint Research Centre (JRC), the European Commission's science and knowledge service. It aims to provide evidence-based scientific support to the European policymaking process. The scientific output expressed does not imply a policy position of the European Commission. Neither the European Commission nor any person acting on behalf of the Commission is responsible for the use that might be made of this publication. For information on the methodology and quality underlying the data used in this publication for which the source is neither Eurostat nor other Commission services, users should contact the referenced source. The designations employed and the presentation of material on the maps do not imply the expression of any opinion whatsoever on the part of the European Union concerning the legal status of any country, territory, city or area or of its authorities, or concerning the delimitation of its frontiers or boundaries.

Contact information

Name: Tomasz Bednarek

Address: European Commission, Joint Research Centre (JRC), Westerduinweg 3, NL-1755 LE Petten

Email: Tomasz.Bednarek@ec.europa.eu

Tel.: +31 224565447

EU Science Hub

<https://ec.europa.eu/jrc>

JRC123219

EUR 30592 EN

PDF

ISBN 978-92-76-30231-5

ISSN 1831-9424

doi:10.2760/83818

Luxembourg: Publications Office of the European Union, 2021

© European Union, 2021



The reuse policy of the European Commission is implemented by the Commission Decision 2011/833/EU of 12 December 2011 on the reuse of Commission documents (OJ L 330, 14.12.2011, p. 39). Except otherwise noted, the reuse of this document is authorised under the Creative Commons Attribution 4.0 International (CC BY 4.0) licence (<https://creativecommons.org/licenses/by/4.0/>). This means that reuse is allowed provided appropriate credit is given and any changes are indicated. For any use or reproduction of photos or other material that is not owned by the EU, permission must be sought directly from the copyright holders.

All content © European Union, 2021

How to cite this report: Bednarek T., Tsoitridis G., *Development of reference hardware for a harmonised testing of PEM single fuel cells*, EUR 30592 EN, Publication Office of the European Union, Luxembourg, 2021, ISBN 978-92-76-30231-5 (online), doi:10.2760/83818 (online), JRC123219.

Contents

Acknowledgment.....	1
Abstract	2
1 Introduction	3
2 Design Assumptions.....	6
2.1 Design criteria.....	6
2.2 Operating conditions.....	6
2.3 Test bench specification.....	8
3 Reference Hardware for harmonised PEM single cell testing	8
3.1 MEA.....	10
3.2 JRC ZERO7CELL assembly	10
3.3 MEA compression	14
3.4 Instrumentation.....	16
4 Experimental validation of the JRC ZERO7CELL	20
5 Conclusions.....	26
References	27
List of abbreviations and definitions	29
List of figures	30
List of tables	31



Acknowledgment

This work has been carried out under the Framework Contract between the Joint Research Centre and the Fuel Cells and Hydrogen 2 Joint Undertaking (FCH2JU).

Authors

Tomasz Bednarek

Georgios Tsotridis

Abstract

This report presents the design of a new hardware for testing performance and durability of single proton exchange membrane (PEM) fuel cells, more specifically their Membrane Electrode Assembly (MEA).

It is well known that testing hardware configurations and working conditions have an influence on the results of the testing. The same MEA, tested by different hardware, will show different performance results. Therefore, the same MEA tested in different laboratories may show different performance depending on the testing hardware used as well as the test protocol employed.

The already existing testing hardware setups for active area of at least 10 cm² are based on single-serpentine, multi-serpentine, interdigitated or mixed flow fields. None of them ensures uniform working conditions in terms of pressure, temperature and concentration of reactants across the active area.

The testing hardware proposed in this report is designed to allow a reliable inter-comparison of test results between different test centres. It aims at operating conditions as far as possible uniform across the MEA active area. This is done by minimising the contribution of the specific hardware setup features on the experimental results. The condition to achieve this is a uniform distribution of all relevant physical quantities of reactant species, such as flow velocity, pressure, temperature and species concentration. However, the operating conditions for tests at a single cell level are still representative to the one for real, commercial fuel cell setups. Also important is that the compression of the tested MEA is well controlled during the whole performance/durability test. Finally, it is important to clarify that the proposed testing hardware is not designed for establishing advanced flow fields with the purpose of improving the performance of a single cell.

The testing hardware design was initiated based on a request from automotive original equipment manufacturers (OEMs) in the frame of the Working Group on harmonisation of PEM fuel cells for automotive application of the Fuel Cells and Hydrogen second Joint Undertaking (FCH2JU).

The report provides a detailed description of the testing hardware design, and the results of its validation experiments.

1 Introduction

Single cell PEM fuel cell experiments are performed for material research as well as for material screening test purposes before scaling-up to short-stack or commercial stack size level. The size of a single cell testing hardware normally varies from 10 cm² up to 25 cm². Currently many commercial single cell testing hardware setups exist, for example provided by Electrochem, Fuel Cell Technologies (FCT), TANDEM Technologies, balticFuelCells and Pragma. In addition to these products, many laboratories use their own in-house built hardware, usually targeting detailed evaluation of specific aspects, such as assessment of electric resistance and contact losses between fuel cell components (Ihonen et al., 2001; Makkus et al., 2000; Miachon and Aldebert, 1995), various flow field patterns (Uchida et al., 1995; Hogarth et al., 1997; Nguyen, 1996; Cooper et al., 2016; Liu et al., 2014; Zehtabiyani-Rezaie et al., 2017) and investigation of the gradients of the physical quantities, such as voltage, current density and temperature, across the active area using segmented current collectors (Scholta et al., 2006; Pérez et al., 2011). Various proposals of fuel cell hardware aiming single-cell or short-stack testing are also presented in (Scholta et al., 2004; Weng et al., 2007; Aicher et al., 2006; Nikiforow et al., 2018; Arisetty et al., 2017).

The Japan Automobile Research Institute (JARI) took an effort in designing the JARI standard single cell (Hashimasa, 2002). Although JARI standard single cell demonstrated good repeatability and reproducibility of experimental results, JARI cell cannot guarantee uniform distribution of physical quantities across the active area of the MEA.

In fact, each single cell testing hardware setup has its own specific flow field which affects the results. Therefore, comparison of experimental results obtained using different testing setups becomes a very challenging endeavour.

Therefore, JRC has taken an effort and leadership role in designing reference test hardware for forthcoming harmonised single PEM fuel cell testing protocol for automotive applications. The activity was initiated based on a request from automotive OEMs at a meeting held in Brussels on 27th June 2016¹.

The design criteria and requirements as well as the various design steps were discussed and agreed with a working group of European partners: CIEMAT, INTA, ISE, KIT, SCHAEFFLER, TECNALIA, JMFC, IRD, FUMATECH, NPL, DLR, PSI, ZPT, SGL, ZSW, TU GRAZ, UBir, CTU, UL, POLIMI and UWAR. Details of all partners are listed in Table 1.













JRC has communicated the proposed solutions to the group in meetings that took place in Brussels on 3rd April 2017 and 23rd October 2017². The participants have agreed on the design assumptions and the proposed features of the new reference hardware. All design criteria and requirements are addressed, as agreed by the above partners, and fulfilled by the testing hardware presented in this report.


The following sections of the report contain the description and experimental validation results of the proposed reference hardware. As all physical quantities across the active area of the cell meet near-zero gradient conditions, the hardware is hereafter called the JRC ZEROVCELL.

⁽¹⁾ European Commission reference number ARES (2017) 1032861.

⁽²⁾ Minutes of the meetings available under European Commission reference numbers: ARES (2017) 2785055 and ARES (2017)6121300 respectively.

Table 1. List of working group partners

 <p>CIEMAT Centro de Investigaciones Energéticas, Medioambientales y Tecnológicas</p>	CIEMAT	Centro de Investigaciones Energéticas, Medioambientales y Tecnológicas
 <p>INSTITUTO NACIONAL DE TÉCNICA AEROSPAZIAL</p>	INTA	Instituto Nacional de Técnica Aeroespacial
 <p>Fraunhofer ISE</p>	ISE	Fraunhofer-Institut für Solare Energiesysteme
 <p>KIT Karlsruhe Institute of Technology</p>	KIT	Karlsruher Institut für Technologie
 <p>SCHAEFFLER</p>	SCHAEFFLER	Schaeffler AG
 <p>tecnalia Inspiring Business</p>	TECNALIA	Tecnalia Research & Innovation Fundazioa
 <p>JM Johnson Matthey Inspiring science, enhancing life</p>	JMFC	Johnson Matthey Plc.
 <p>IRD IRD Fuel Cells</p>	IRD	IRD Fuel Cells A/S
 <p>fumatech Funktionelle Membranen und Anlagentechnologie BWT GROUP</p>	FUMATECH	FUMATECH BWT GmbH
 <p>NPL</p>	NPL	National Physical Laboratory
 <p>DLR</p>	DLR	Deutsche Zentrum für Luft- und Raumfahrt
 <p>PAUL SCHERRER INSTITUT PSI</p>	PSI	Paul Scherrer Institute

	ZBT	Zentrum für BrennstoffzellenTechnik GmbH
	SGL	SGL Group - The Carbon Company
	ZSW	Zentrum für Sonnenenergie- und Wasserstoff-Forschung Baden-Württemberg
	TU GRAZ	Technische Universität Graz
	UBir	University of Birmingham
	CTU	České vysoké učení technické v Praze
	UL	Université de Lorraine
	POLIMI	Politecnico di Milano
	UWAR	University of Warwick

2 Design Assumptions

2.1 Design criteria

The criteria, agreed by the working group partners³, met by the JRC ZEROVCELL are the following:

- 10 cm² active area.
- Straight parallel gas channels representative for automotive fuel cell flow fields.
- Stoichiometric and constant gas flow regimes of humidified reactants (air and H₂).
- co- as well as counter-flow of reactants.
- At 4.0 Acm⁻² current density steady operation:
 - Laminar flow regime (Reynolds number, $Re < 1,000$).
 - Reactant pressure drop across active area (anode and cathode) less than 10.0 kPa.
 - Temperature variation ± 1.0 °C across the active area.
 - The average change (integrated over the surface perpendicular to the gas flow) of gas composition less than 10% difference between inlet and outlet for both reactants.

As a parallel reactants flow field configuration is employed in the JRC ZEROVCELL, uniform inlet conditions are assumed for all channels regarding:

- pressure,
- mass flow rate,
- gas composition and
- temperature

The results presented in section 4 demonstrate through polarisation curve that the JRC ZEROVCELL meets the requirements of laminar flow, temperature variation and pressure drop.

2.2 Operating conditions

For the operation of the JRC ZEROVCELL it was agreed to use as far as possible the harmonised operating conditions representative for automotive applications (Tsotridis et al., 2015). However, small gas flows, corresponding to air and fuel stoichiometry, $\lambda_{H_2}=1.3$ and $\lambda_{O_2}=1.5$ respectively, given in (Tsotridis et al., 2015), are not applicable to the parallel channel currently employed in the JRC ZEROVCELL. This is due to redistribution of the gas flow among a large number of parallel channels. Hence, the mass flow per channel would be much lower compared to that in a single serpentine channel commonly used in single cell PEM fuel cell test hardware setups. Therefore the operating cathode and anode stoichiometry ratios need to be adjusted.

According to the design criteria (section 2.1) the average reactant gas composition difference between the gas inlet and outlet should not differ by more than 10%. Since the concentration of hydrogen fuel does not change along the channels, this constrain corresponds to the cathode compartment only. Hence, the cathode oxidant stoichiometry needs to be $\lambda_{O_2} \geq 10$. However, too high air flow may violate the required laminar flow regime ($Re < 1000$) and cause an increase of the pressure drop across the active area. Therefore, oxidant stoichiometry is set to $\lambda_{O_2} = 10$.

³ Minutes of the meetings available under European Commission reference numbers: ARES (2017) 2785055 and ARES (2017)6121300.

Therefore, the fuel stoichiometry for the JRC ZEROVCELL is thus increased to $\lambda_{H_2}=8$, resulting in a pressure drop similar to that in the cathode compartment (according to calculations using the Darcy-Weisbach formula, see section 4.4).

The operating conditions are listed in Table 2.

Table 2. Operating conditions for JRC ZEROVCELL.

Parameter		Operating conditions		
		Symbol	Unit	Setting
	Nominal cell operating temperature	T_{cell}	°C	80
ANODE	Fuel gas inlet temperature	$T_{fuel,in}$	°C	85
	Fuel gas inlet relative humidity*	$RH_{fuel,in}$	%	100
	Fuel gas inlet pressure (absolute)	$P_{fuel,in}$	kPa	250
	Fuel inlet stoichiometry	λ_{H_2}	–	8.0
CATHODE	Oxidant gas inlet temperature	$T_{ox,in}$	°C	85
	Oxidant gas inlet relative humidity*	$RH_{ox,in}$	%	100
	Oxidant gas inlet pressure (absolute)	$P_{ox,in}$	kPa	230
	Oxidant inlet stoichiometry	λ_{Ox}	–	10.0

*Inlet gas relative humidity is related to operating temperature of the cell.

Source: JRC, 2018

2.3 Test bench specification

The test bench requirements are listed in Table 3.

Table 3. Test stand requirements for JRC ZEROVCELL single cell configuration.

Parameter	Unit	Min	Max	Protection Limit
General				
Number of load banks		1	-	
Number of power supplies		1	-	
Current	A	0	100	
Heat removal	W	0	100	
Pressure difference between the fuel and oxidant	kPa	0	50	80
Pressure difference between coolant circuit and anode&cathode compartments	kPa	0	300	
Compressed air	kPa	500	3000	
Fuel (Anode) Stream				
Inlet gas temperature	°C	20	95	100
Inlet relative humidity	%	0	100	
Inlet pressure (relative)	kPa	10	200	300
Outlet pressure (relative)	kPa	10	200	300
Anode flow (dry)	l min ⁻¹	0.05	10	
Anode pressure difference between cell inlet and outlet	kPa	0	60	
Oxidant (Cathode) Stream				
Inlet gas temperature	°C	20	95	100
Inlet relative humidity	%	0	100	
Inlet pressure (relative)	kPa	10	200	300
Outlet pressure (relative)	kPa	10	200	300
Cathode flow (dry)	l min ⁻¹	0.05	20	
Cathode pressure difference between cell inlet and outlet	kPa	0	80	
Coolant (DI water) to Hardware Stream				
Inlet pressure	kPa	0	200	300
Coolant flow rate	l min ⁻¹	1	3	
Inlet and Outlet temperature	°C	40	90	95
Pressure difference between inlet and outlet	kPa	0	40	
Coolant electric conductivity	μS cm ⁻¹	0	100	

Source: JRC, 2020

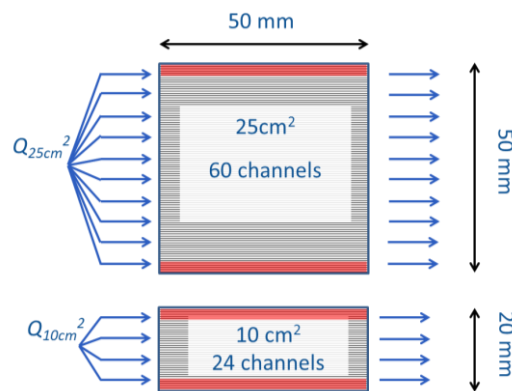
3 Reference Hardware for harmonised PEM single cell testing

For each reactant, the total gas channel length is 100 mm while the active area length of the JRC ZEROVCELL is 50 mm.

Since each of the parallel channel is exposed to the same inlet conditions, the number of channels (determining the width of the active area) has no effect on the obtained results. Therefore, by varying the active area width, the JRC ZEROVCELL is capable of accommodating a range of active area sizes, from 10 cm² (2x5 cm) up to 25 cm² (5x5 cm), as can be seen in Figure 1.

The size and shape of the gas manifolds are such that uniform conditions are ensured for all channels. Due to the active area length and uniform inlet conditions at the beginning of active area, the results obtained from tests performed using different active area sizes will be directly comparable.

Figure 1. Scaling of active area of the JRC ZEROVCELL; arrows indicate gas flow direction.

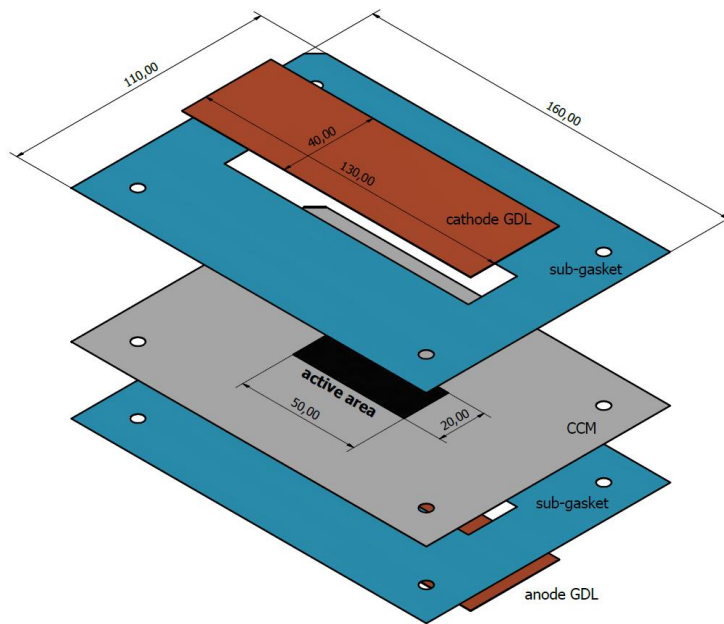


Source: JRC, 2018

3.1 MEA

The drawing of a 10 cm² active area MEA is shown in Figure 2.

Figure 2. Assembly of 10 cm² MEA for JRC ZEROVCCELL.



Source: JRC, 2020

The MEA is composed of the following parts:

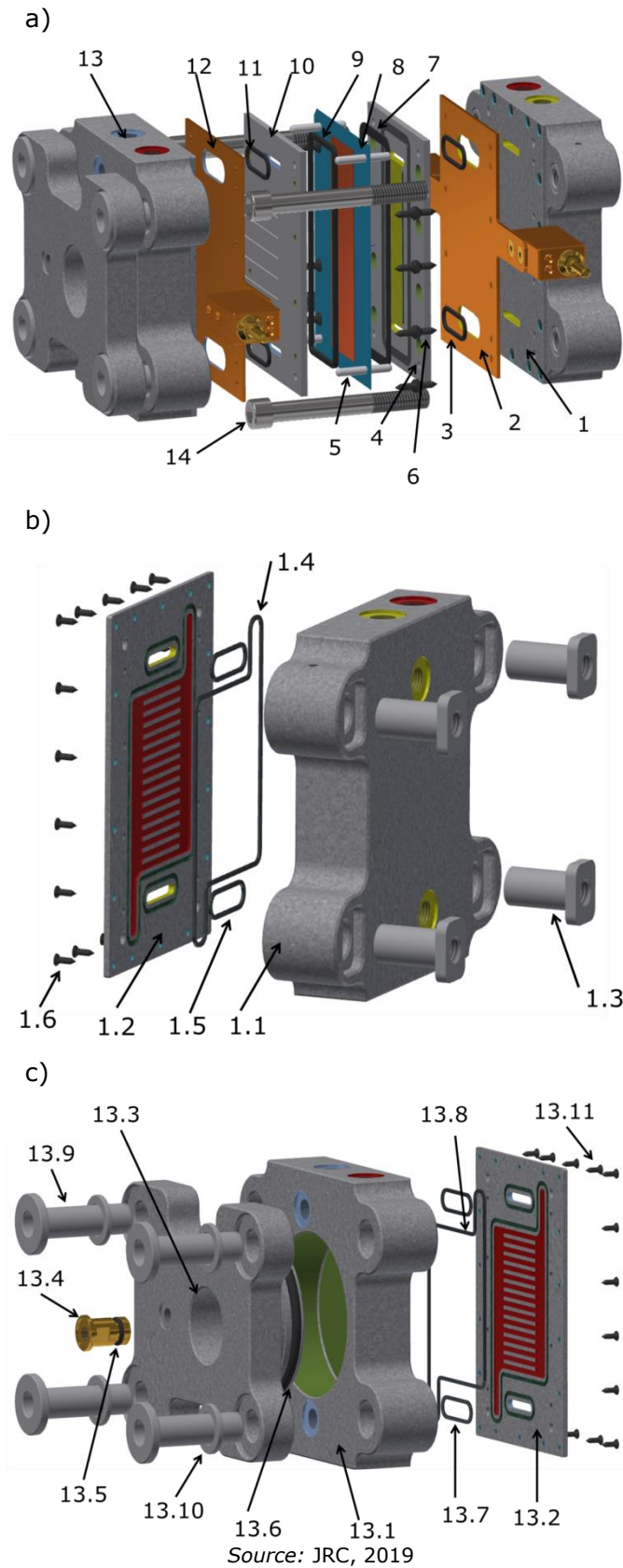
- Catalyst Coated Membrane (CCM).
- Anode and cathode sub-gaskets reinforcing the edges of the MEA making it easier to handle and more resistant to mechanical damage.
- Gas Diffusion Layers (GDL) providing reactants to the CCM and collecting electric current.

3.2 JRC ZEROVCCELL assembly

The JRC ZEROVCCELL assembly is presented in Figure 3. For the gas and coolant connections G1/4" quick-fittings are used. The compression chamber as well as coolant, anode and cathode compartments are coloured as follows:

- yellow – anode gas inlet/outlet, anode compartment
- blue – cathode gas inlet/outlet, cathode compartment
- red – coolant inlet/outlet, coolant circuit
- green – compression chamber of pneumatic pressurising system.

Figure 3. JRC ZEROVCELL assembly: a) full view, b) anode end-plate unit and c) cathode end-plate unit.



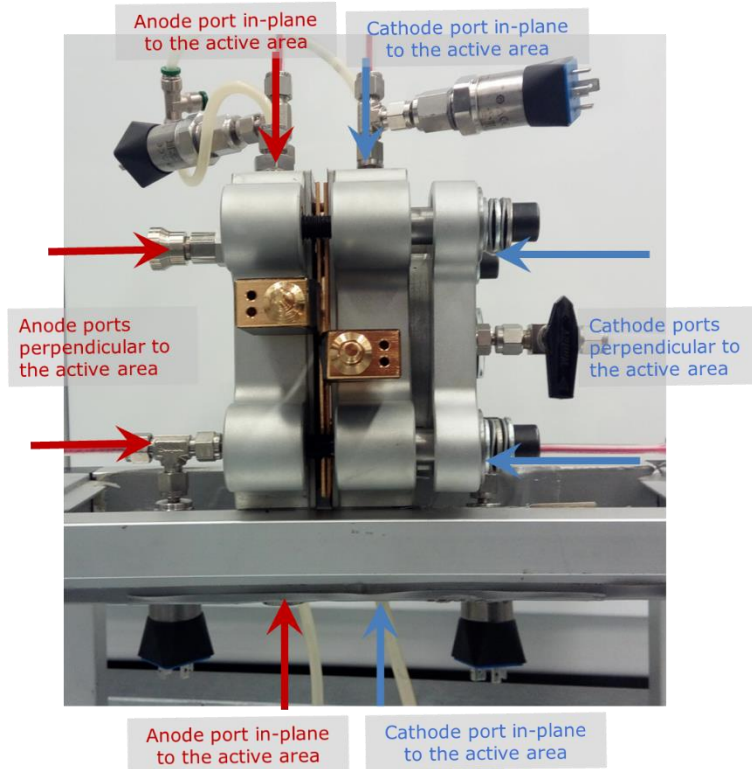
JRC ZEROVCELL components, listed in Figure 3 is as follows:

1. Anode end-plate unit (Figure 3a):
 - 1.1. Main anode end-plate, aluminium alloy grade AW 2024, anodised (Figure 3b)
 - 1.2. Anode end plate lid, aluminium alloy grade AW 2024, anodised (Figure 3b)
 - 1.3. Nut, 4 pcs, brass or galvanised steel (Figure 3b)
 - 1.4. Coolant circuit sealing, 1 pcs, o-ring 1.78x126.72 70NBR (Figure 3b)
 - 1.5. Gas sealing, 2 pcs, o-ring 1.78x26.7 70NBR (Figure 3b)
 - 1.6. Fixing screws, 18 pcs, M3x10, flat head, stainless steel (Figure 3b)
2. Anode current collector, copper, gold plated $>5\mu\text{m}$ (Figure 3a)
3. Gas sealing, 2 pcs, o-ring 2.62x26.64 70 NBR (Figure 3a)
4. Anode bi-polar plate, graphite grade FC-GR347B (Figure 3a)
5. Positioning pin, 4 pcs, nylon (Figure 3a)
6. Fixing screws, 16 pcs, M4x12 flat head, nylon (Figure 3a)
7. Anode MEA sealing, 1 pcs, custom made, silicon shore 35-50 (Figure 3a)
8. MEA (Figure 3a)
9. Cathode MEA sealing – 1 pcs, custom made, silicon shore 35 or x-ring 2.62x107.63 70 NBR (Figure 3a)
10. Cathode bi-polar plate, graphite grade FC-GR347B (Figure 3a)
11. Gas sealing, 2 pcs, o-ring 2.62x26.64 70 NBR (Figure 3a)
12. Cathode current collector, copper gold coated $>5\mu\text{m}$ (Figure 3a)
13. Cathode end-plate unit (Figure 3a)
 - 13.1. Main cathode end-plate, aluminium alloy grade AW 2024, anodised (Figure 3c)
 - 13.2. Cathode end-plate lid, aluminium alloy grade AW 2024, anodised (Figure 3c)
 - 13.3. Cathode pressurising plate, aluminium alloy grade AW 2024, anodised (Figure 3c)
 - 13.4. Pressure gauge fitting for compression chamber – custom made, brass, circlip 16mm (Figure 3c)
 - 13.5. Sealing of pressure gauge fitting, 1 pcs, o-ring 2.62x10.77 70NBR, back-up ring 11.2x15.5x1.2 PTFE (Figure 3c)
 - 13.6. Sealing of compression chamber, 1 pcs, x-ring 5.33x81.92 70 NBR, back-up ring 82.2x91x2.0 PTFE, use vacuum sealing grease (Figure 3c)
 - 13.7. Gas sealing, 2 pcs, o-ring 1.78x26.7 70NBR (Figure 3c)
 - 13.8. Coolant circuit sealing, 1 pcs, o-ring 1.78x126.72 70NBR (Figure 3c)
 - 13.9. Bolt sleeve, 4 pcs, brass or stainless steel (Figure 3c)
 - 13.10. Fixing washer, 4 pcs, brass or stainless steel; 4 pcs, circlip 17mm (Figure 3c)
 - 13.11. Fixing screws, 18 pcs, M3x10, stainless steel (Figure 3c)
14. Clamping bolt, M12x120, hex socket cap, 4 pcs; dome spring washer, 8 pcs; regular washer 12 pcs (Figure 3a)
15. Fittings (not shown in Figure 3):
 - 15.1. Gas inlet/outlet fittings, G1/4", 8 pcs.
 - 15.2. Coolant inlet/outlet fittings, G1/4", 4 pcs.
 - 15.3. Compressed air port, G1/8", valve, 1 pcs.
16. Pressure gauge for compression chamber (not shown in Figure 3), 0-30 bar, G1/8"

The JRC ZEROVCELL is symmetric, hence all gas manifolds can be considered as inlet or outlet manifolds depending on the employed flow direction, co- or counter-flow. Each of the four gas manifolds of the JRC ZEROVCELL, namely cathode inlet manifold, cathode outlet manifold, anode inlet manifold and anode outlet manifolds, have two G1/4" gas ports.

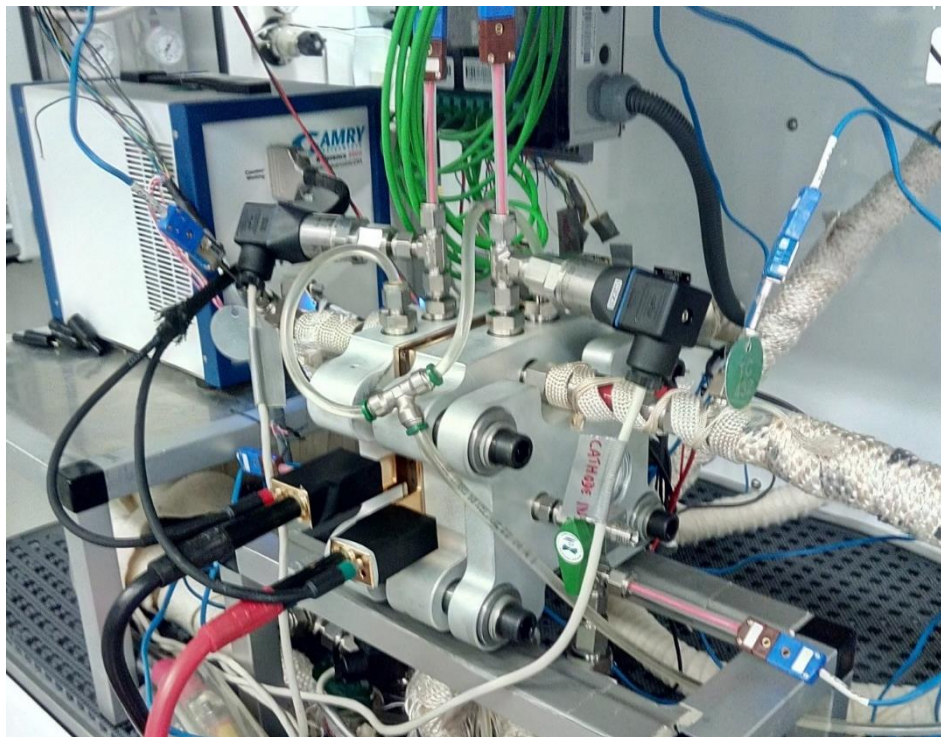
For every manifold one port is in-plane of the MEA, the other is perpendicular, as shown in Figure 4. Both ports in each manifold can be used either as gas inlet/outlet or housing for additional sensors in gas manifolds, depending on cell orientation and experiment needs.

Figure 4. Localisation of inlet/outlet ports to the gas manifolds.



Source: JRC, 2019

Figure 5. JRC ZEROCELL installed on a test bench.



Source: JRC, 2019

The JRC ZEROVCELL installed on a test bench is shown in Figure 5.

In addition to the design criteria given in section 2.1, the following is addressed by the JRC ZEROVCELL:

- MEA compression system is embedded in the hardware. Compression may be applied using compressed air and/or bolts. In case of lack of compressed air, bolts can be used to apply pressure in compression chamber.
- Compression of the MEA may be adjusted during cell testing if needed.
- Independent cooling circuits (self-venting) for anode and cathode sides.
- Gas lines and cooling circuits fittings G $\frac{1}{4}$, quick-fitting can be employed.
- Additional sensors (i.e. pressure transducers, thermocouples, humidity sensors etc.) can be embedded in the gas manifolds inside the testing hardware.
- MEA is sealed by hardware embedded sealing, adjustable to the various thickness of MEA.
- Cell voltage terminals are separated from current terminals.

3.3 MEA compression

The compression system is embedded in the JRC ZEROVCELL. It consists of an end plate with compression chamber (green) and a floating pressurising plate piston – elements 13.1 and 13.3 in Figure 3c. The clamping force is applied by the gas pressure in the compression chamber. It can be charged by compressed air supplied externally.

In the absence of an external supply of compressed air, MEA compression can be applied manually by clamping bolts, see Figure 6. The maximum pressure in compression chamber is 30 bar. The actual pressure in compression chamber can be monitored by a pressure gauge (see Figure 6).

Due to the floating pressurising plate, it is not required to apply the same torque at all four clamping bolts. However, the position of the piston with respect to the cathode end plate should be kept parallel with 5mm tolerance, as shown in Figure 6.

The diameter of the circular compression chamber (green element 13.3 in Figure 3c) is 91 mm. Therefore, 1 bar (100 kPa) of pressure is turned into a clamping force of ~650N. However, due to the relatively large GDLs only part of the total clamping force is applied to the active area of the MEA.

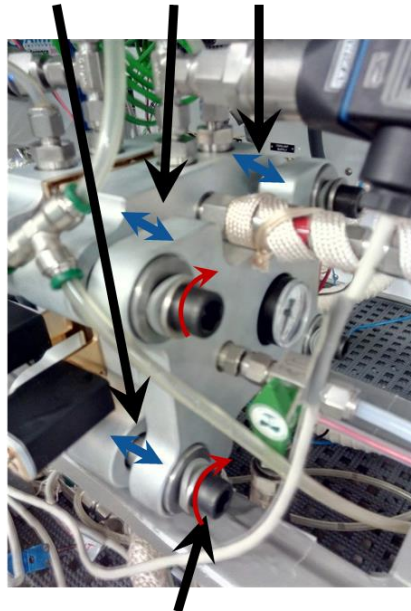
Assuming 10cm² active area size and negligible contribution of the sealing gaskets, the ratio of the area of lands⁴ at cathode side to the total area of bi-polar plate in contact with the GDL is 276:3311. Therefore, 1 bar of pressure in the compression chamber is turned into ~54 N of force applied to the active area, equivalent to GDL compression of 54 kPa (0.55 kg cm⁻²).

The above considerations are rough estimation of the clamping force acting on the active area in relation to the pressure inside the compression chamber. If the MEA manufacturer does not recommend GDL compression, spacers can be used to limit the compression of the GDL to the desired thickness, as presented in Figure 7.

(⁴) Land – the rib between two gas channels within the bi-polar gas flow plates.

Figure 6. Cathode end-plate unit with embedded pneumatic compression hardware.

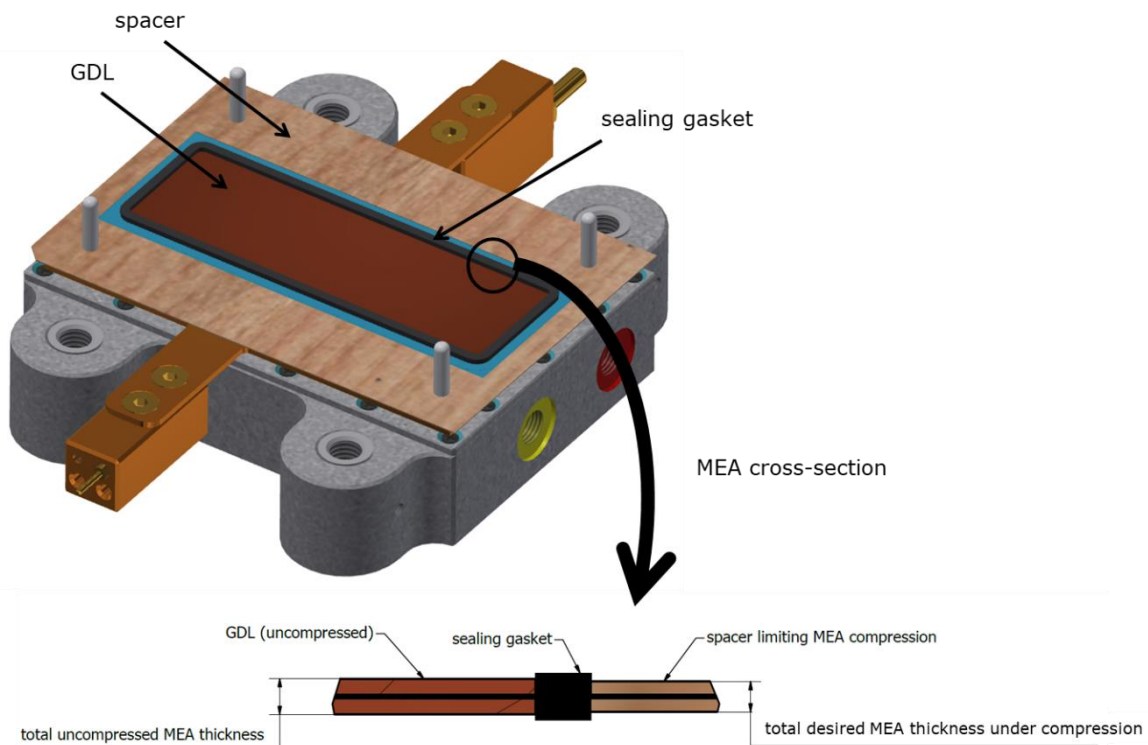
Distance between main cathode end-plate (13.1) and pressurising plate (13.3) should be uniform $\pm 5\text{mm}$



Clamping bolt

Source: JRC, 2019

Figure 7. Positioning of spacers limiting GDL compression.

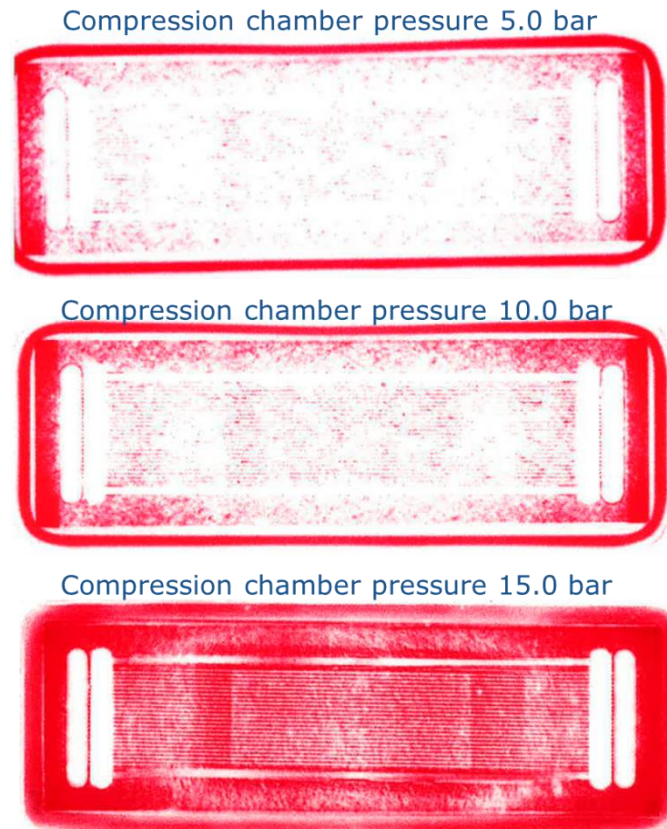


Source: JRC, 2020

A uniform MEA compression at the active area provides uniform distribution of electric and thermal contact resistances. A pressure sensitive Fuji Film LLW (Super Low Pressure) was used to examine MEA compression uniformity at pressures of 5, 10 and 15 bar.

The results of the compression tests are presented in Figure 8 showing a rather uniform clamping pressure across the active area as well as inlet and outlet zones.

Figure 8. MEA compression test using pressure sensitive Fuji Film LLW.



Source: JRC, 2019

3.4 Instrumentation

The JRC ZEROVCELL houses embedded sensors as follows:

- 10 thermocouples (TCs) located in the bi-polar plates for independent measurement of temperature distribution across the active area: 5 TC at anode side and 5 TC at cathode side.
- 4 additional ports allow placing sensors (i.e. thermocouples, humidity sensors etc.) inside the gas manifolds, as close as possible to the gas channels inlet/outlet to the manifolds. Because of this positioning the sensor measurements are minimally affected by the presence of accumulated liquid water.
- 4 absolute and 2 differential pressure transducers allowing to achieve accurate gas pressure in the JRC ZEROVCELL inside the gas manifolds, for anode and cathode compartments independently.

The position of thermocouples inside the testing hardware is shown in Figure 9. The thermocouples are located inside the bi-polar plates, 3mm from GDL – bi-polar plate interface providing information on temperature distribution along the gas channels. The grooves for the thermocouples are perpendicular to the direction of the flow in the gas channels allowing to move the respective TC along the width of the active area during testing.

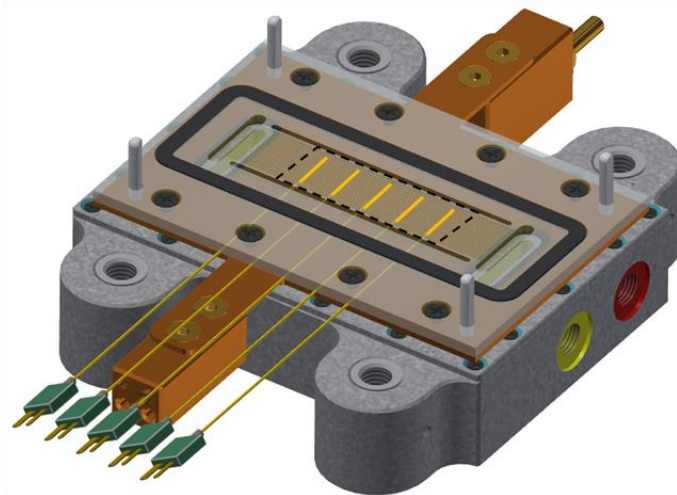
As shown in Figure 9, the 5 TCs at each side are located:

- at the beginning of active area,
- at 25% of the active area length,
- in the middle of active area,
- at 75% of the active area length and
- at the end of active area.

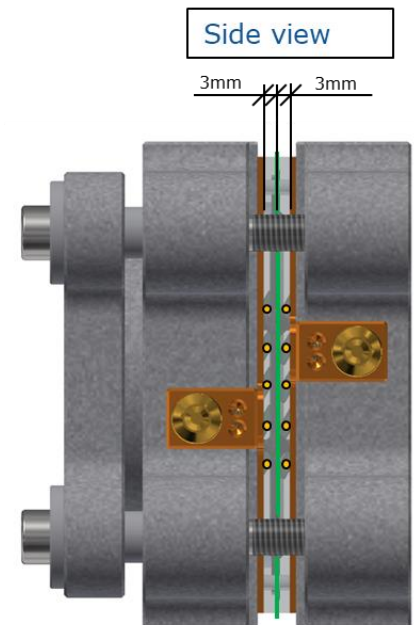
Figure 9. Location of thermocouples inside JRC ZERO7CELL.

Position of thermocouples (yellow)
5 anode and 5 cathode (10 in total):

- **Beginning of active area**
- **25% of total active area length**
- **50% of total active area length**
- **75% of total active area length**
- **End of active area**

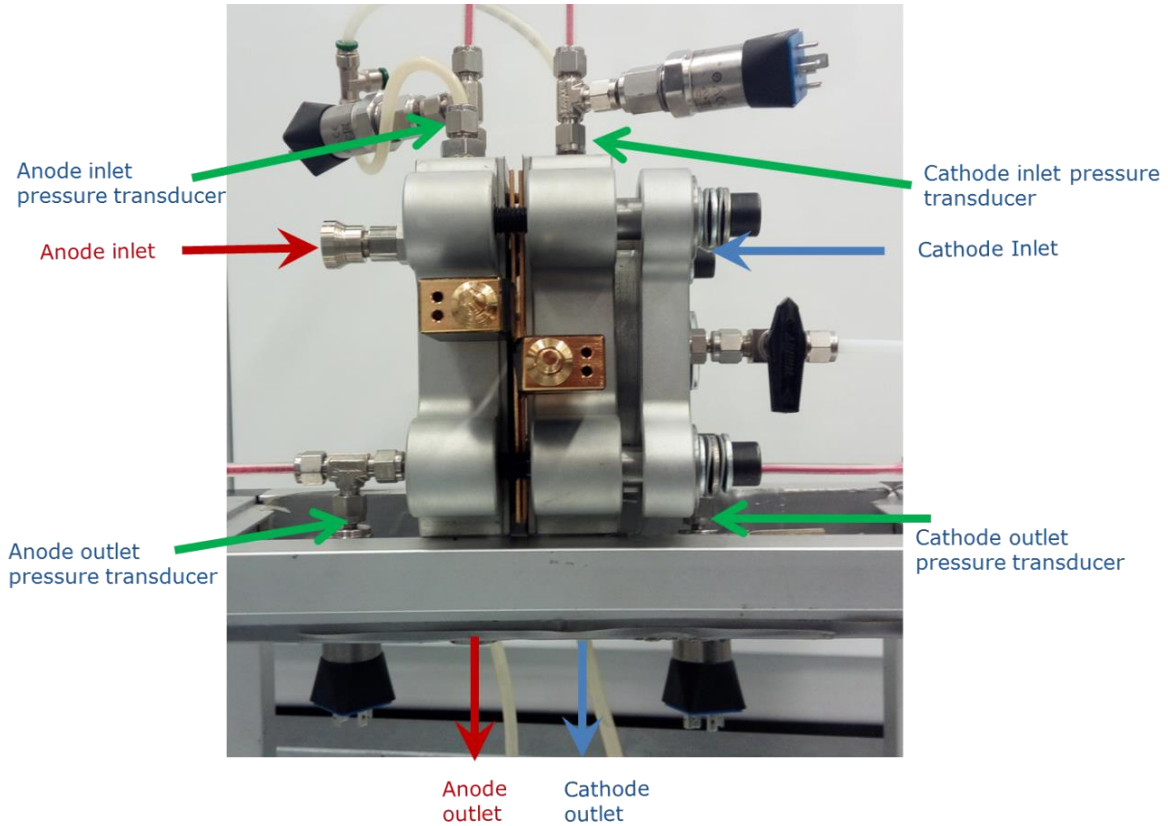


Position of thermocouples inside
graphite bi-polar plates, 3mm
from MEA.



Source: JRC, 2020

Figure 10. Location of pressure transducers in the JRC ZEROCELL, vertical cell orientation.



Source: JRC, 2019

Four pressure transducers are located in the gas inlet and outlet sensor ports as shown in Figure 10. Their position allows to measure the pressure in the gas manifolds without disturbance by gas lines or fittings.

Since the presence of transducers affects the gas flow in the channels, there is no possibility to place pressure transducers at the beginning and the end of the active area. Instead, pressures at the beginning and the end of active area are calculated as follows:

$$p_{begin} = p_{inlet} - \Delta p_{inlet} \quad (2)$$

$$p_{end} = p_{outlet} + \Delta p_{exit} \quad (3)$$

where p_{begin} and p_{end} are pressures at the beginning and at the end of the active area, p_{inlet} and p_{outlet} are measured pressures at inlet and outlet of the testing hardware. Δp_{inlet} and Δp_{exit} are the pressure drop in respectively the inlet and outlet zones estimated from the Darcy-Weisbach formula (Landau and Lifshitz, 1987)

$$\Delta p_{inlet/exit} = \frac{59 \mu v l_{inlet/outlet}}{2D^2} \quad (4)$$

where: v is average velocity of the gas, $l_{inlet/outlet}$ is length of inlet/outlet zone, μ is the dynamic viscosity of the humidified gas and D is the hydraulic diameter of the gas channel. Values of μ and v are calculated from the inlet gas properties, applied mass flow rate and channel cross-section. The hydraulic diameter D of the channel is calculated as follows

$$D = \frac{4A}{P} \quad (5)$$

where A is the channel cross-section and P is its perimeter.

Since the analytically pressure drop calculated using Eqn (4) does not account for liquid water effects, this approach is conservative. Therefore, the pressure drop within the active the area is not larger than

$$\Delta p = p_{begin} - p_{end} \quad (6)$$

4 Experimental validation of the JRC ZEROVCCELL

A testing campaign was performed to validate the JRC ZEROVCCELL. The results demonstrate that the JRC ZEROVCCELL meets the design criteria for 10 cm² active area MEA. For comparison a single cell testing hardware with 25 cm² single-serpentine gas channel was used as a reference, Figure 11.

The performance is evaluated by means of polarisation curves (cell voltage versus current density).

Figure 11. 25 cm² active area PEM fuel cell with single-serpentine flow field. The channel geometry is as follows: channel width 1 mm, channel depth 1 mm, pitch 2 mm.



Source: JRC, 2018

Two types of MEA were used in the validation tests; details are listed in Table 4. Both MEAs are composed of different components showing possible application of the JRC ZEROVCCELL for typical MEAs for stationary (MEA1) and high performance transport applications (MEA2).

Table 4. Specification of used MEAs.

	MEA1	MEA2
Active area size	10 cm ² , 20x50 mm	10 cm ² , 20x50 mm
Membrane thickness	28 μm	18 μm
Anode catalyst	Pt, loading 0.3 mg cm ⁻²	Pt, loading 0.1 mg cm ⁻²
Cathode catalyst	Pt, loading 0.3 mg cm ⁻²	Pt, loading 0.4 mg cm ⁻²
Anode GDL	Sigracet GDL 29BC	Sigracet GDL 25BC
Cathode GDL	Sigracet GDL 29BC	Sigracet GDL 25BC
Sealing gasket material	VITON	VITON

Source: JRC, 2019

Polarisation curves for MEA1 and MEA2 are shown in Figure 12 and Figure 13 respectively. For both MEAs, the polarisation curves obtained using the JRC ZEROVCELL show a linear behaviour in a wide range of current densities ($\sim 1 \text{ A cm}^{-2}$) up to $\sim 3 \text{ A cm}^{-2}$.

This indicates that mass transport limitations caused by diffusion of reactants and liquid water presence are negligible compared to the ohmic losses which is an inherited property of the tested MEA. Such feature of the JRC ZEROVCELL shows the possibility of examining the performance of a tested MEA up to $\sim 3 \text{ A cm}^{-2}$ in linear regime without visible effects caused by reactant mass transport.

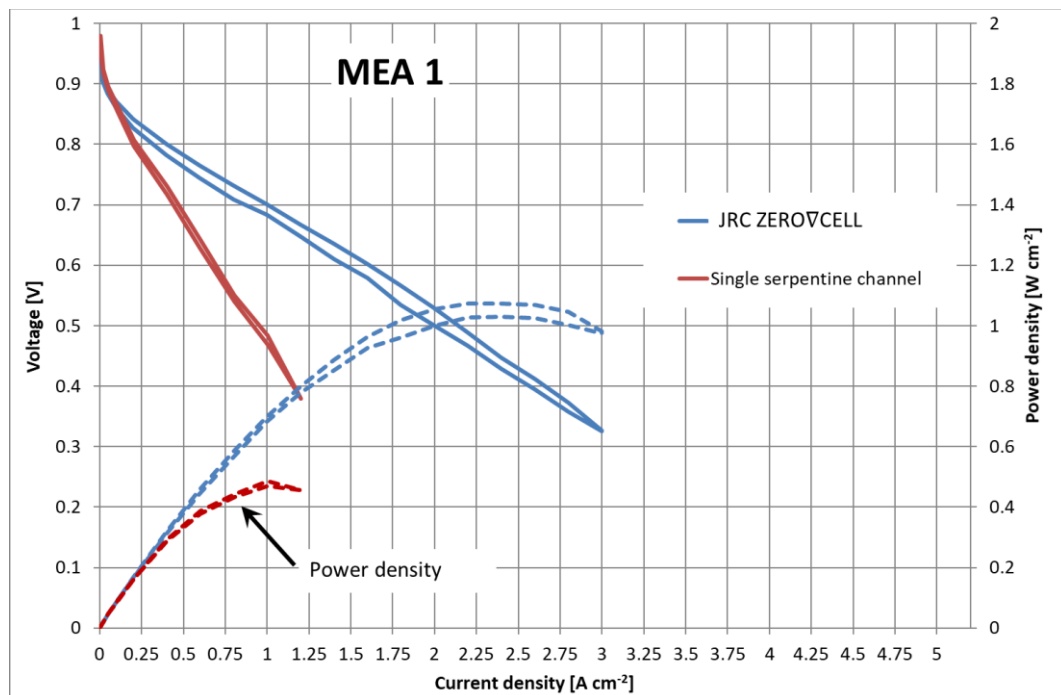
For MEA1 the maximum power density obtained using JRC ZEROVCELL is $\sim 1.1 \text{ W cm}^{-2}$ at a current density of $\sim 2.25 \text{ A cm}^{-2}$. Whereas the performance obtained by a single-serpentine testing hardware is only $\sim 0.5 \text{ W cm}^{-2}$ ($\sim 0.5 \text{ V}$ at $\sim 1.0 \text{ A cm}^{-2}$).

During the validation experiment with the high performance MEA2 (Figure 13), the JRC ZEROVCELL provides a much greater performance of $\sim 1.9 \text{ W cm}^{-2}$ at a current density of 3.8 A cm^{-2} , which is twice as high as that is obtained from the same MEA tested using a test hardware with single serpentine flow pattern ($\sim 0.95 \text{ W cm}^{-2}$, Figure 13).

The JRC ZEROVCELL is versatile to test MEAs with different properties, such as thickness, catalyst loading etc. From the results presented in Figure 12 and Figure 13 it is obvious that the JRC ZEROVCELL shows considerably higher performance than the single serpentine hardware using the same MEA1 and MEA2.

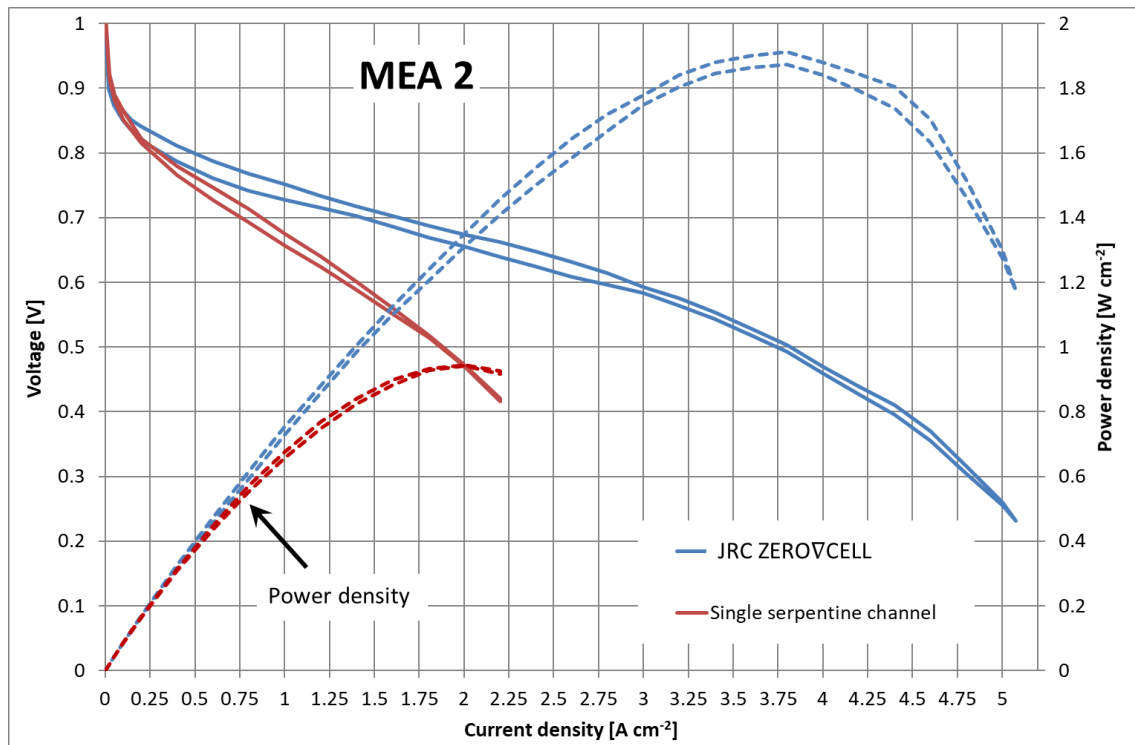
At current densities above 3 A cm^{-2} (MEA2, Figure 13) the polarisation curve bends down showing that mass transport limitations become dominant. However, the operation of the JRC ZEROVCELL is still stable without significant fluctuations of performance and working conditions as shown in the evolution plots of voltage, pressure and temperature (Figure 14 to Figure 16). Therefore, the JRC ZEROVCELL allows for investigation of MEA limitation of 1) ohmic resistance losses, 2) reactants mass transport and 3) product water removal from catalyst to gas channel, over a wide range of current densities.

Figure 12. Polarisation curves obtained using a single serpentine hardware and the JRC ZEROVCELL – MEA1.



Source: JRC, 2019

Figure 13. Polarisation curves obtained using a single serpentine hardware and the JRC ZEROVCELL – MEA 2.



Source: JRC, 2019

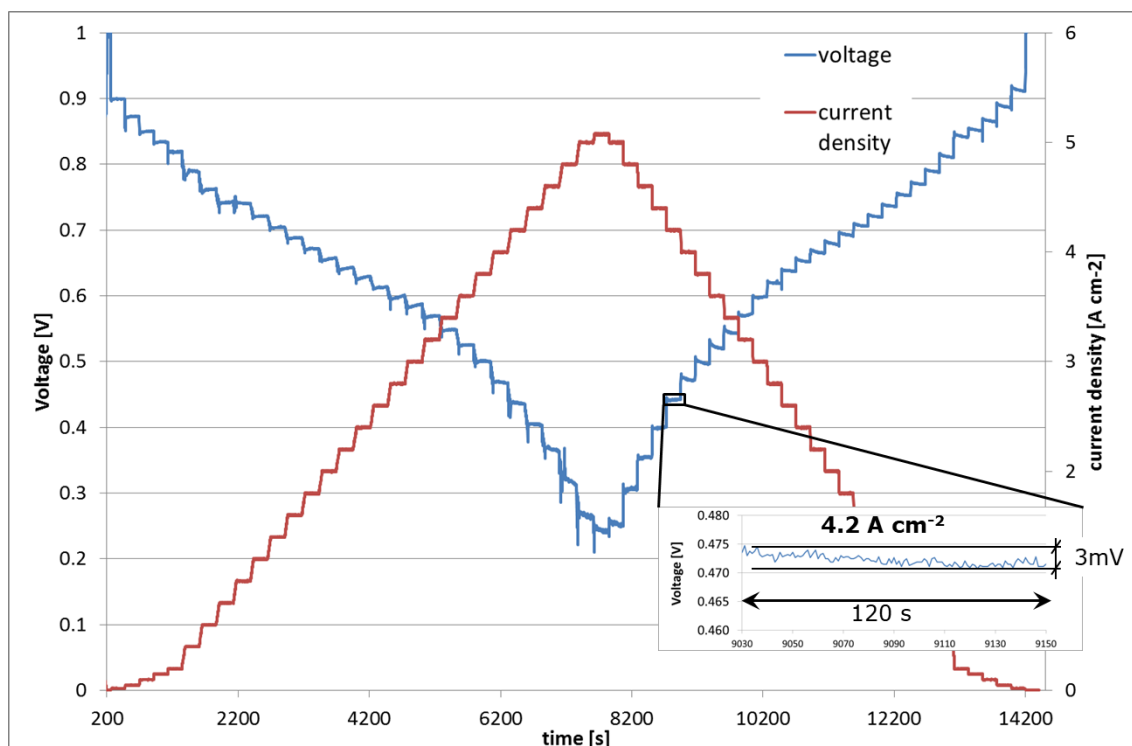
Voltage evolution during the polarisation test using JRC ZEROVCELL for MEA2 going up to current density of 5 A cm⁻² is presented in Figure 14.

In the polarisation test each step of current density lasts for 210 s (3 min 30 s), whereas the voltage measurement is averaged over the last 30 s of the step. Besides some voltage spikes due to change of the electric current generated by the electronic load, the voltage during the last 60 s of each polarisation curve current density step is stable with very low voltage fluctuations.

For example, the voltage evolution at current density 4.2 A cm⁻² over the last 120 s (2 min) of the time step is zoomed (Figure 14) revealing a variation of +/-1.5 mV which is very close to the accuracy of the test bench measurement instrumentation (1.0 mV).

Since the effects of liquid water (sudden blocking and unblocking of gas channels by water droplets) would result in significant voltage fluctuations, no disturbances due to liquid water being present are visible.

Figure 14. Voltage evolution during polarisation test with zoom-in showing voltage fluctuations during 120 s at high current density.

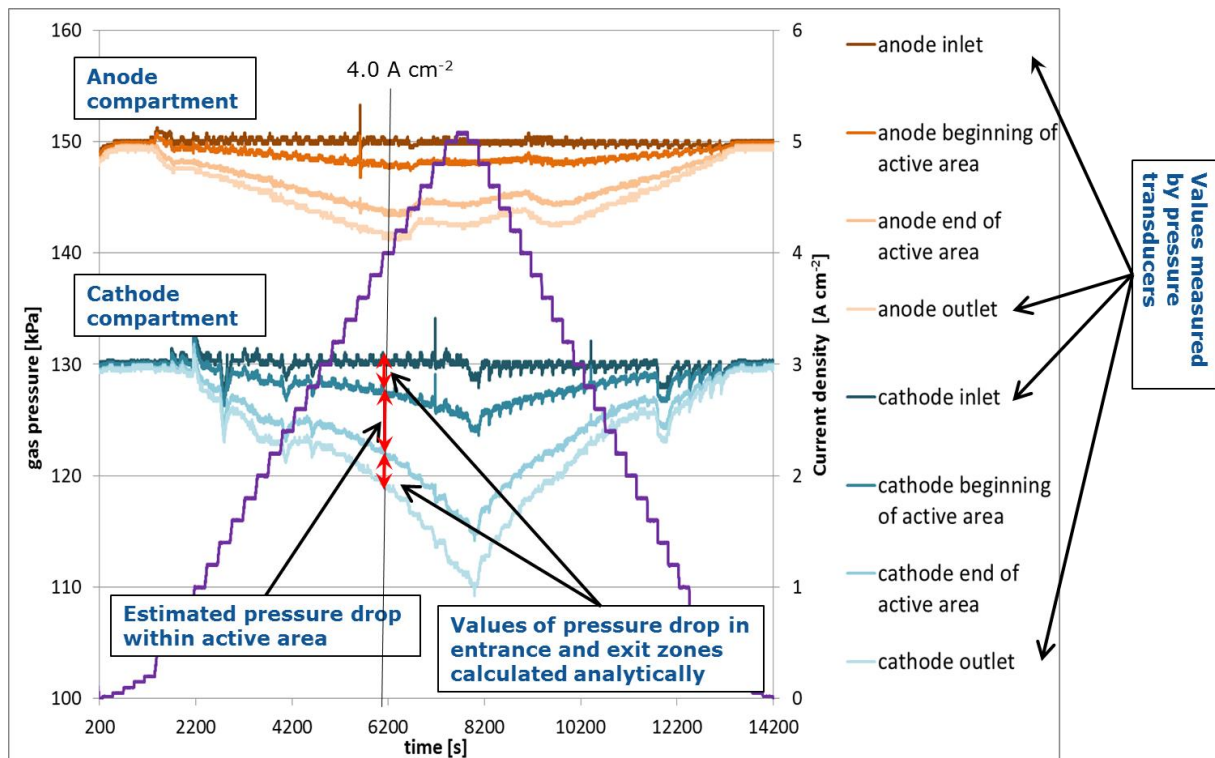


Source: JRC, 2019

The evolution of gas pressure during a polarisation test using the JRC ZEROVCELL on MEA2 is presented in Figure 15. At the design point of 4 A cm^{-2} the pressure drop within the active area does not exceed 7 kPa in the cathode and 5 kPa in the anode compartments, meeting the requirement of a maximum pressure drop across the active area of 10 kPa at 4 A cm^{-2} . Some pressure fluctuations in the cathode compartment at 1.5 A cm^{-2} current density (at $\sim 2,200 \text{ s}$ and $\sim 12,200 \text{ s}$ of test duration, Figure 15) correspond to switching of air mass flow controller operation. Note, in order to increase flow accuracy, two different flow controllers are used namely one for flow below 1.5 NL min^{-1} (0.025 NL s^{-1}) and one for flow above 1.5 NL min^{-1} .

As the evolution of the pressure drop is proportional to the current density and no significant fluctuations are observed, it is concluded that laminar flow prevails in the gas channels even at a current density of 5 A cm^{-2} .

Figure 15. Anode and cathode gasses pressure evolution during polarisation curve experiment using the JRC ZEROVCELL with MEA2.



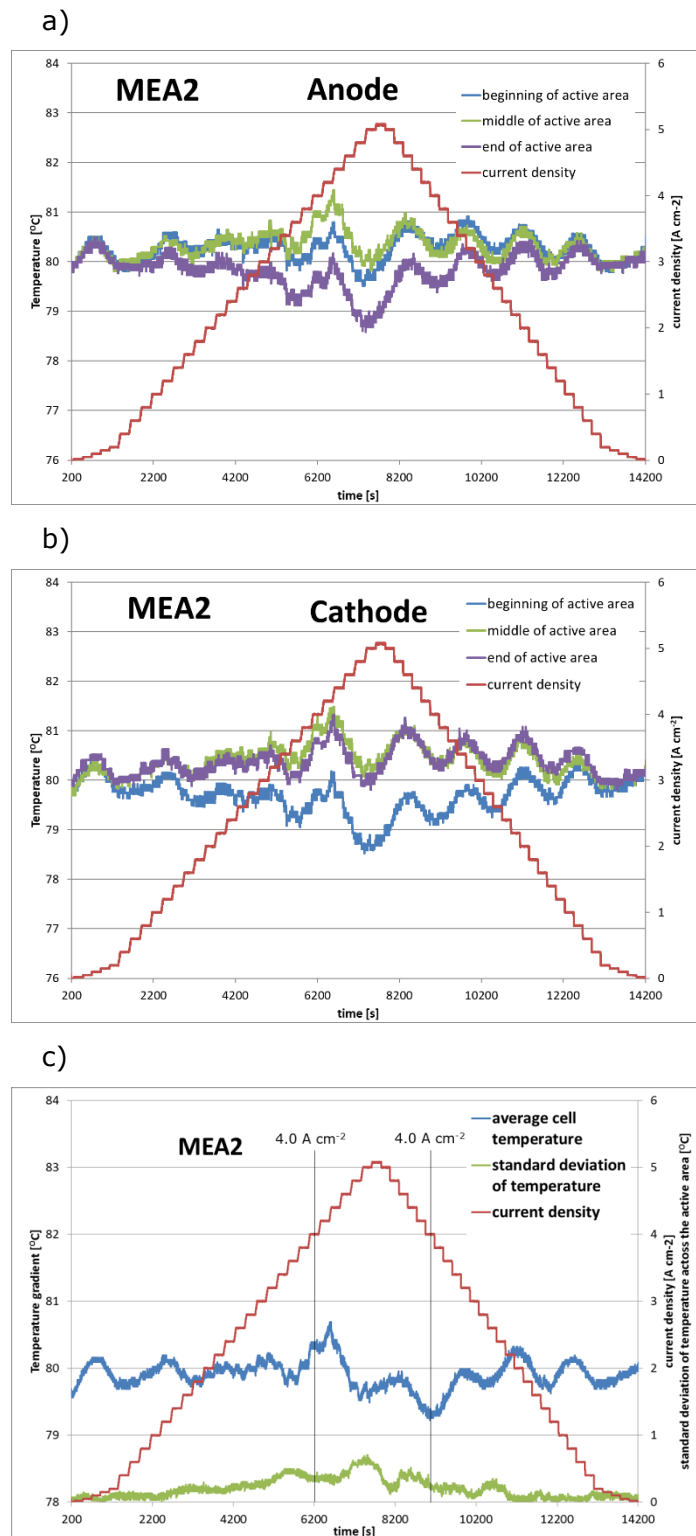
Source: JRC, 2019

The evolution of temperature of the JRC ZEROVCELL during the polarisation experiment is presented in Figure 16. In order to make plots clearer and easier for interpretation, the values of temperature are given in 3 (out of possible 5) locations at anode and cathode compartments, namely: beginning, middle and end of the active area, presented in Figure 16a and Figure 16b. The standard deviation of the temperature measured by all 10 thermocouples located in both compartments across the active area is presented in Figure 16c. The sinusoidal fluctuation of temperature is due to the test coolant (de-ionised water) flow control using a chiller.

Because the response of the chiller is much slower than changes due to current density steps, the control algorithm must anticipate future requirement for cooling down the cell. Consequently, the cell temperature oscillates around the set operating temperature. This behaviour can be further improved by better temperature control of the coolant liquid at the bench level and is independent on the cell hardware.

In the whole range of applied current densities, up to 5.0 A cm^{-2} , the standard deviation (Figure 16c) does not exceed 1°C even considering fluctuations due to the chiller's temperature control, thus fulfilling the design requirement $\pm 1.0^\circ\text{C}$. At the design current density of 5.0 A cm^{-2} the temperature standard deviation is $\sim 0.5^\circ\text{C}$.

Figure 16. Temperature evolution during polarisation test using MEA2 using JRC ZEROCELL: a) anode compartment, b) cathode compartment, c) average and standard deviation of temperature across the active area.



Source: JRC, 2019

5 Conclusions

The proposed reference hardware for testing a PEM Single Cell, called also JRC ZEROVCELL, allows performing experiments in both co- and counter-flow modes in vertical MEA orientation.

It is equipped with additional sensor ports allowing measurements directly in the gas manifolds of the JRC ZEROVCELL, i.e. reactant gas pressure, temperature, humidity etc. The operating temperature of the cell is measured by 10 TCs located in the anode and cathode bi-polar plates. Temperature measurements demonstrate that for the design current density of 5 A cm^{-2} , the temperature gradient across the length and width of the active area does not exceed $\pm 1.0^\circ\text{C}$ and the pressure drop over the active area is smaller than the design limit of 10 kPa.

The experimental results presented in Section 4 show that the proposed JRC ZEROVCELL provides results of the required quality with low fluctuations of the measured quantities, namely: cell voltage, pressure in all 4 inlet/outlet manifolds and temperature across the active area. Therefore, the JRC ZEROVCELL provides improved quality of the experimental data and facilitates accurate comparisons of test results.

The polarisation curve obtained using MEA2 shows linear ohmic behaviour up to $\sim 3 \text{ A cm}^{-2}$. The maximum electric power density reaches a value of $\sim 1.9 \text{ W cm}^{-2}$, while the maximum current density is as high as 5 A cm^{-2} at $\sim 0.25 \text{ V}$. This shows that the proposed JRC ZEROVCELL allows exposing tested MEA to very high current densities with minimal effects of liquid water being present in the gas channels.

Therefore, the JRC ZEROVCELL testing hardware allows characterisation of MEA components in a more reliable way than done so far. It also enables more quantitative assessment of the overall technological progress in the field of PEM fuel cells used in both, automotive applications and stationary applications.

The JRC ZEROVCELL is made available to the research community and industry upon request and subject to a Non-Disclosure Agreement (NDA), while an *open-source hardware* licence is in preparation at the time of publishing of this report.

References

- Aicher, T., B. Lenz, F. Gschnell, U. Groos, F. Federici, L. Caprile, and L. Parodi, 'Fuel Processors for Fuel Cell APU Applications', *Journal of Power Sources*, Vol. 154, No. 2, March 21, 2006, pp. 503–508. DOI:10.1016/J.JPOWSOUR.2005.10.026.
- Arisetty, S., J. Rock, J. Dabel, B. Lakshmanan, E. Kjell, C. Kennette, M. DeBolt, et al., 'Development of a Common Differential Fuel Cell Test Fixture and Protocols to Expedite Material Development', *Meeting Abstracts*, Vol. MA2017-02, No. 32, September 1, 2017, pp. 1400–1400.
- Cooper, N.J., T. Smith, A.D. Santamaria, and J.W. Park, 'Experimental Optimization of Parallel and Interdigitated PEMFC Flow-Field Channel Geometry', *International Journal of Hydrogen Energy*, Vol. 41, No. 2, January 12, 2016, pp. 1213–1223. DOI:10.1016/j.ijhydene.2015.11.153.
- Hashimasa, Y., 'Development of JARI Standard Single Cell for Testing Cell Materials', *JARI Research Journal*, Vol. 24, 2002, pp. 455–458.
- Hogarth, M., P. Christensen, A. Hamnett, and A. Shukla, 'The Design and Construction of High-Performance Direct Methanol Fuel Cells. 2. Vapour-Feed Systems', *Journal of Power Sources*, Vol. 69, No. 1–2, November 1, 1997, pp. 125–136. DOI:10.1016/S0378-7753(97)02581-0.
- Ihonen, J., F. Jaouen, G. Lindbergh, and G. Sundholm, 'A Novel Polymer Electrolyte Fuel Cell for Laboratory Investigations and In-Situ Contact Resistance Measurements', *Electrochimica Acta*, Vol. 46, No. 19, June 15, 2001, pp. 2899–2911. DOI:10.1016/S0013-4686(01)00510-2.
- Landau, L.D., and E.M. Lifshitz, *Fluid Mechanics*, Edited by McGraw-Hill, Image Rochester NY, Vol. 6, Vol. 6, *Course of Theoretical Physics*, Pergamon Press, 1987. DOI:10.1007/b138775.
- Liu, H., P. Li, D. Juarez-Robles, K. Wang, and A. Hernandez-Guerrero, 'Experimental Study and Comparison of Various Designs of Gas Flow Fields to PEM Fuel Cells and Cell Stack Performance', *Frontiers in Energy Research*, Vol. 2, 2014, p. 2.
- Makkus, R.C., A.H. Janssen, F.A. de Bruijn, and R.K.A. Mallant, 'Use of Stainless Steel for Cost Competitive Bipolar Plates in the SPFC', *Journal of Power Sources*, Vol. 86, No. 1–2, March 1, 2000, pp. 274–282. DOI:10.1016/S0378-7753(99)00460-7.
- Miachon, S., and P. Aldebert, 'Internal Hydration H₂/O₂ 100 Cm² Polymer Electrolyte Membrane Fuel Cell', *Journal of Power Sources*, Vol. 56, No. 1, July 1, 1995, pp. 31–36. DOI:10.1016/0378-7753(95)80005-2.
- Nguyen, T. V., 'A Gas Distributor Design for Proton-Exchange-Membrane Fuel Cells', *Journal of The Electrochemical Society*, Vol. 143, No. 5, May 1, 1996, p. L103. DOI:10.1149/1.1836666.
- Nikiforow, K., J. Pennanen, J. Ihonen, S. Uski, and P. Koski, 'Power Ramp Rate Capabilities of a 5 kW Proton Exchange Membrane Fuel Cell System with Discrete Ejector Control', *Journal of Power Sources*, Vol. 381, March 31, 2018, pp. 30–37. DOI:10.1016/J.JPOWSOUR.2018.01.090.
- Pérez, L.C., L. Brandão, J.M. Sousa, and A. Mendes, 'Segmented Polymer Electrolyte Membrane Fuel Cells—A Review', *Renewable and Sustainable Energy Reviews*, Vol. 15, No. 1, January 2011, pp. 169–185. DOI:10.1016/j.rser.2010.08.024.
- Scholta, J., N. Berg, P. Wilde, L. Jörissen, and J. Garche, 'Development and Performance of a 10 KW PEMFC Stack', *Journal of Power Sources*, Vol. 127, No. 1–2, March 10, 2004, pp. 206–212. DOI:10.1016/J.JPOWSOUR.2003.09.040.
- Scholta, J., F. Häussler, W. Zhang, L. Küppers, L. Jörissen, and W. Lehnert, 'Development of a Stack Having an Optimized Flow Field Structure with Low Cross Transport Effects', *Journal of Power Sources*, Vol. 155, No. 1, April 18, 2006, pp. 60–65.
- Tsotridis, G., A. Pilenga, G. De Marco, and T. Malkow, 'EU Harmonised Test Protocols for PEMFC MEA Testing in Single Cell Configuration for Automotive Applications', *JRC Science for Policy Report, EUR 27632 EN*, 2015. DOI:10.2790/54653.
- Uchida, M., Y. Aoyama, N. Eda, and A. Ohta, 'New Preparation Method for Polymer-Electrolyte Fuel Cells',



Journal of The Electrochemical Society, Vol. 142, No. 2, February 1, 1995, p. 463.
DOI:10.1149/1.2044068.

Weng, F.-B., B.-S. Jou, A. Su, S.H. Chan, and P.-H. Chi, 'Design, Fabrication and Performance Analysis of a 200W PEM Fuel Cell Short Stack', *Journal of Power Sources*, Vol. 171, No. 1, September 2007, pp. 179–185.
DOI:10.1016/j.jpowsour.2006.12.061.

Zehtabiyani-Rezaie, N., A. Arefian, M.J. Kermani, A.K. Noughabi, and M. Abdollahzadeh, 'Effect of Flow Field with Converging and Diverging Channels on Proton Exchange Membrane Fuel Cell Performance', *Energy Conversion and Management*, Vol. 152, November 15, 2017, pp. 31–44.
DOI:10.1016/J.ENCONMAN.2017.09.009.

List of abbreviations and definitions

CCM	Catalyst Coated Membrane
EU	European Union
FCH2JU	Fuel Cells and Hydrogen Second Joint Undertaking
GDL	Gas Diffusion Layer
JARI	Japan Automobile Research Institute
JRC	Joint Research Centre
MEA	Membrane Electrode Assembly
NDA	Non-Disclosure Agreement
OEM	Original Equipment Manufacturer
PEM	Polymer Electrode Membrane, Proton Exchange Membrane
Re	Reynolds number
TC	thermocouple

List of figures

Figure 1. Scaling of active area of the JRC ZEROVCELL; arrows indicate gas flow direction.	9
Figure 2. Assembly of 10 cm ² MEA for JRC ZEROVCELL.....	10
Figure 3. JRC ZEROVCELL assembly: a) full view, b) anode end-plate unit and c) cathode end-plate unit.	11
Figure 4. Localisation of inlet/outlet ports to the gas manifolds.	13
Figure 5. JRC ZEROVCELL installed on a test bench.	13
Figure 6. Cathode end-plate unit with embedded pneumatic compression hardware.	15
Figure 7. Positioning of spacers limiting GDL compression.	15
Figure 8. MEA compression test using pressure sensitive Fuji Film LLW.	16
Figure 9. Location of thermocouples inside JRC ZEROVCELL.....	17
Figure 10. Location of pressure transducers in the JRC ZEROVCELL, vertical cell orientation.	18
Figure 11. 25 cm ² active area PEM fuel cell with single-serpentine flow field. The channel geometry is as follows: channel width 1 mm, channel depth 1 mm, pitch 2 mm.....	20
Figure 12. Polarisation curves obtained using a single serpentine hardware and the JRC ZEROVCELL – MEA1.	21
Figure 13. Polarisation curves obtained using a single serpentine hardware and the JRC ZEROVCELL – MEA 2.	22
Figure 14. Voltage evolution during polarisation test with zoom-in showing voltage fluctuations during 120 s at high current density.....	23
Figure 15. Anode and cathode gasses pressure evolution during polarisation curve experiment using the JRC ZEROVCELL with MEA2.....	24
Figure 16. Temperature evolution during polarisation test using MEA2 using JRC ZEROVCELL: a) anode compartment, b) cathode compartment, c) average and standard deviation of temperature across the active area.....	25



List of tables

Table 1. List of working group partners.....	4
Table 2. Operating conditions for JRC ZEROVCELL.....	7
Table 3. Test stand requirements for JRC ZEROVCELL single cell configuration.....	8
Table 4. Specification of used MEAs.....	20



GETTING IN TOUCH WITH THE EU

In person

All over the European Union there are hundreds of Europe Direct information centres. You can find the address of the centre nearest you at: https://europa.eu/european-union/contact_en

On the phone or by email

Europe Direct is a service that answers your questions about the European Union. You can contact this service:

- by freephone: 00 800 6 7 8 9 10 11 (certain operators may charge for these calls),
- at the following standard number: +32 22999696, or
- by electronic mail via: https://europa.eu/european-union/contact_en

FINDING INFORMATION ABOUT THE EU

Online

Information about the European Union in all the official languages of the EU is available on the Europa website at: https://europa.eu/european-union/index_en

EU publications

You can download or order free and priced EU publications from EU Bookshop at: <https://publications.europa.eu/en/publications>. Multiple copies of free publications may be obtained by contacting Europe Direct or your local information centre (see https://europa.eu/european-union/contact_en).

The European Commission's science and knowledge service

Joint Research Centre

JRC Mission

As the science and knowledge service of the European Commission, the Joint Research Centre's mission is to support EU policies with independent evidence throughout the whole policy cycle.



EU Science Hub

ec.europa.eu/jrc



@EU_ScienceHub



EU Science Hub - Joint Research Centre



Joint Research Centre



EU Science Hub



Publications Office
of the European Union

doi:10.2760/83818

ISBN 978-92-76-30231-5